RSC Advances

ROYAL SOCIETY OF CHEMISTRY

www.rsc.org/advances

Waterborne Biodegradable Polyurethane 3-Dimentional Porous Scaffold For Rat Cerebral Tissue Regeneration

Yan-Chao Wang[a,1], Fang Fang[a,1,*]Ying-Ke Wu[b], Xiao-Lin Ai[a,] Ting Lan[c], Rui-Chao Liang[a], Yu Zhang[d], Narasimha Murthy Trishul [a], Min He[a], Chao You[a], Chuan Yu [e] and Hong Tan[b,*]

a Department of Neurosurgery, West China Hospital, Sichuan University, Chengdu,610041, Sichuan, People's Republic of China.

b College of Polymer Science and Engineering, State Key Laboratory of Polymer Materials Engineering, Sichuan University, Chengdu 610065, People's Republic of China.

c Department of Pathology, West China Hospital, Sichuan University, Chengdu,610041, Sichuan, People's Republic of China.

d Department of Neurosurgery, Affiliated Hospital/Clinical Medical College of Chengdu University, Chengdu,610081, Sichuan, People's Republic of China.

e State Key Laboratory of Biotherapy and Cancer Center, West China Hospital, Sichuan University, Chengdu 610041, People's Republic of China

This work was financially supported by the projects of National Natural Science Foundation of China (contract/grant number: 81100925, 81472361, 51273124, 51273126) and the National Science Fund for Distinguished Young Scholars of China (contract/grant number: 51425305)

[1] **First Author:** Fang Fang contributed equally to this work with Yan-Chao Wang, and is the co-first author for this paper.

***Corresponding authors:** Fang Fang and Hong Tan.

Tel.: +86-28-85460961; fax: +86-28-85405402.

E-mail addresses: merrisn@hotmail.com and wyc89890707@icloud.com (F. Fang); hongtan@scu.edu.cn (H. Tan).

Abstract

Rehabilitation of traumatic brain injury (TBI) is a significant challenge for neurosurgeons as no effective strategies for cerebral tissue reconstruction can be adopted in clinical applications. To explore an appropriate method for cerebral tissue regeneration, we have developed a kind of waterborne biodegradable polyurethane (WBPU) 3-dimentional (3D) porous scaffold. We have prepared two kinds of WBPU (WBPU17 and WBPU25) 3D scaffolds based on different molar content of poly ethylene glycol (PEG) within scaffolds. The porosity of WBPU17 and WBPU25 scaffolds is 83.29±0.53% and 86.72±0.78% respectively. While, the mean pore size of WBPU17 scaffold and WBPU25 scaffold is 20.10μm and 22.18μm, respectively. No pronounced cytotoxicity was noticed for rat's glial cells when treated with degradation liquid of WBPU17 and WBPU25 scaffold. What is more, both WBPU17 and WBPU25 scaffolds treaded groups showed stronger expression of neuronal growth associated protein (GAP43) and synaptophysin, indicating better nerve regeneration in experiment groups than none scaffold control group in rat's TBI model. Besides, functional recovery also displayed satisfactory result in WBPU17 and WBPU25 scaffold treaded group. Overall, WBPU25 scaffold has better performance than WBPU17 scaffold. These results of our experiment proved that WBPU 3D

porous scaffold, especially WBPU25 scaffold, is a promising therapeutic implant for both cerebral tissue regeneration and neural functional recovery in TBI.

Key words: Waterborne Biodegradable Polyurethane 3-dimentional Porous Scaffold; Traumatic brain injury; Nerve regeneration; Axonal regeneration

1. introduction

Traumatic brain injury (TBI) is a common disease in neurosurgery. It can cause contusion and laceration of brain as well as intracranial hematoma that leads to high morbidity and mortality[1, 2]. To increase patient's survival rate, the main clinical strategy to treat severe TBI is decompressive craniotomy, in which case, some necrotic brain tissue is often excised. However, abscission of cerebral tissue will cause massive loss of nervous tissue especially the axons and neurons[3-5]. When the injury is located in the cerebral eloquent areas, such as motor center, it may lead to paralysis of corresponding muscle and bring grievous outcome. The main purpose for treatment of TBI is to promote regeneration of brain tissue and reconstruction of axon and synapses to achieve tissue repair and neural functional rehabilitation[1, 6]. To improve the outcome of TBI patients, numerous remarkable works have been attempted. For example, nerve growth factor (NGF) has been applied to treat TBI since its discovery. Although NGF shows promising effects, it can only bring limited functional recovery and incomplete tissue repair[7]. In addition, cell therapy has been applied in TBI treatment,[8] but it was inadequate in the situation of massive loss of nerve tissue[9]. Therefore, until now there are no effective therapies efficacious for the

TBI, and materials that can simultaneously provide fine functional recovery and histic repair are still greatly demanded.

Nanomaterials have been applied in neural tissue engineering study for a quite long time. Now the application of nanomaterials in TBI is mainly focused on three fields, the hydrogels, nanofibers and biodegradable scaffolds[9]. Among these three materials, hydrogel is mostly studied. Hyaluronic acid (HA) hydrogel and its modified products have been reported that they could promote further neurite extension and angiogenesis in rat's TBI model[10-12]. Rutledge *et al* have reported peptide nanofiber scaffold for brain tissue repair and axon regeneration with functional recovery of vision[13]. Although some achievements have been made in investigation of hydrogels and nanofibers to treat brain injury, they still have defects in some aspects such as fast degradation or quite significant toxicity[9]. For the biodegradable nanoscaffold, ideally, the scaffold should be progressively degraded and gradually replaced by the regenerating tissue. Thus, the scaffold can provide enough time to permit cell infiltrate and support axon regrowth, but scaffold should not stay too long to interfere with the extracellular matrix (ECM) deposition and reconnection of axons[9]. Now some *in vivo* studies have shown admirable regeneration effects of biodegradable nanoscaffold on peripheral nerve regeneration. Wang *et al* have reported that electrospuned chitosan scaffold could repair transected sciatic nerve in rats[14]. Other studies have reported that scaffolds prepared by poly(e- caprolactone - co-ethyl ethylene phosphate) (PCLEEP)[15], poly(D,L-lactide-co-glycolic)acid (PLGA) /poly(ε-caprolactone) (PCL)[16] could also bring regeneration of sciatic nerve in rats.

But for the central nerve system regeneration, especially the brain tissue regeneration, effect of biodegradable nanoscaffold is very limited. Park *et al* have implanted neural stem cells seeded polyglycolic acid (PGA)-based scaffold into the cavity resulting from hypoxia/ischemia injury in mice[17]. Tissue regrowth could been observed, but the scaffold hardly lead to full restoration of lost functions. Currently, there are still no strategies for brain tissue reconstruction that have been adopted in clinical applications[9].

Polyurethane is a FDA approved polymer for medical application[18-20]. It have good biocompatibility, and the physical and chemical properties of polyurethane can be designed to meet different requirements by using different composition and synthesis procedure[21]. Polyurethane scaffold has displayed admirable effects in peripheral nerve regeneration and bring both neural repair and functional recovery[22, 23]. In our previous work, we have synthesized waterborne biodegradable polyurethane (WBPU) 3-dimentional (3D) porous scaffolds through technique that has not employed organic solvent. Thus toxicity of the obtained porous scaffolds can be decreased to a greater degree [24, 25]. The WBPU 3D scaffold has shown favorable cell compatibility and biodegradability in human umbilical vein endothelial cells (HUVECs) and leaded to adhesion and proliferation of HUVECs[24]. Toward this rationale, we suppose that the WBPU 3D scaffold may be a good candidate for cerebral tissue regeneration. In this study, we investigated the nerve regeneration effect and toxicity of WBPU 3D scaffold *in vitro* and *in vivo*. Cytotoxicity of WBPU 3D scaffold was tested in rat glial cell by CCK8 assay, and we evaluated tissue

toxicity through observation of the inflammatory reaction by HE stain. Effects of the WBPU 3D scaffold on nerve regeneration were investigated in fields of functional recovery, histological regeneration (Including staining of neurite outgrowth and synapses markers), and western blot analyze observations in rat's TBI model and we used saline as control.

2. Materials and methods

2.1 Preparation and morphology of Waterborne Biodegradable Polyurethane (WBPU) 3-Dimentional porous scaffold

The waterborne biodegradable polyurethane (WBPU) was synthesized via poly ethylene glycol (PEG, molecular weight 1450), poly ε-caprolactone (PCL, molecular weight 2000) and L-lysine, 1,3-propanediol(PDO) and L-lysine diisocyanate (LDI) which were prepared according to pervious report and 3D scaffold porous structure was formed by froze-dry method (Fig S1, See the ECI for detailed information) [24, 25]. We prepared two kinds of different WBPU 3D scaffolds, WBPU17 scaffold and WBPU25 scaffold. The differences between these two scaffolds were the molar content of PEG in soft segment was 17%, 25% respectively. The microstructure of scaffold was examined under scanning electron microscope (SEM, JSM-7500F, Japan) with an accelerating voltage of 15kV. Before morphological observation, the specimens were fractured in liquid nitrogen with a forceps and coated with gold. The scaffolds' pore diameters were calculated by analyzing the SEM images using image-pro plus 6 (USA). The porosity of WBPU 3D scaffold is expressing as

following equation: $\varepsilon_{WBPU} = 1 - \frac{\rho^{*}_{WBPU}}{\rho_{WBPU}}$

Here, ρ^{*}_{WBPU} is the density of the scaffold and ρ_{WBPU} is the density of film.

2.2 In vitro cell culture and CCK-8 assay

Primary cell culture of rat glial cells from one-day old newborn rat was performed. Rat's brain was cut up after removing dura and blood vessels. The tissue was treated with 0.25% trypsin at 37°C for 30min. The dispersed cells were seeded to ploy-L-lysine precoated 6 well plates (cell density 7×10^5 /well). Cells were cultured in Dulbecco's modified eagle medium: nutrient mixture F-12 (DMEM/F-12, Gibico life, USA) supplemented with 10% fetal bovine serum (FBS, Hyclone, USA) and 100U/ml penicillin (Gibico life, USA) and 100U/ml streptomycin (Gibico life, USA) and maintained in a 37°C incubator (Hera Cell, Thermo Scientific) with a humidified 5%CO_2 atmosphere. After two generations cells were seeded in 96-well plates at concentration of 5×10^3 cells per well and incubated for 24h. The logarithmically diluted degradation liquid of WBPU from concentration of 100% to 0.1% (PH 7.4) were then added in 96-well plates at the volume of 10μL per well. After another 24h of incubation, cells in each well were exposed to 10μL CCK-8 solutions (DOJINDO, Japan) and incubated for 4h at 37°C. Lastly, the absorbance of formazan product was measured at 450nm on a microplate reader (DNM-9602, Nanjing Perlove Medical Equipment Co., Ltd., China).

2.3Animal model and surgical procedures

The animal studies were carried out in compliance with Principles of Laboratory Animal Care of National Institute of Health, China and with approval from Ethics

Committee of Sichuan University. We chose thirty SPF adult Sprague Dawley (SD) female rats (Institute of Laboratory Animal of Sichuan Academy of Medical Sciences, Chengdu, China) weighing 200–220 grams to evaluate the effect of nerve regeneration of brain tissue. Rats were housed at temperature of 20–22 °C, relative humidity of 50–60% and 12h artificial light-dark cycles with standard laboratory chow and distilled water freely. All animals would be in quarantine for a week before experiment. The animals were randomly divided into three groups each with ten rats. The effect of brain tissue regeneration of the WBPU25 and WBPU17 scaffold treated groups were compared with the saline groups. The rat's hairs on the head were removed before surgery and we located the body surface symbol of primary motor cortex (M1) on rat's skull followed the stereotaxic coordinates[26]. Each rat was anesthetized with 0.5ml/100g body weight 10% chloral hydrate (*i*p) before operation. We have made a 5mm×4mm circular skull window in front of the bregma and removed the dura. About 4mm×4mm×3mm sized M1 area was resected along the bone window, after resection brain cotton was used to stanch bleeding. The similar size WBPU scaffold was tailored and imbedded in the place of tissue defect while the control group was filled by saline according to routine surgical procedure. Followed the implantation the skin incision was closed with 2-0 silk sutures (Mersilk® Johnson & Johnson, USA). After surgery every animal was administrated cefathiamidine (BYS, China, 0.05g/d, *ip*) for three days to prevent infection and each animal was housed in single cage with free access for food and water. The animals were intensively examined for signs of paralysis and autotomy. At each time interval,

histomorphometric and neural functional analysis were performed to evaluate the efficiency of WBPU 3D scaffold for brain tissue regeneration.

2.4Functional assessment of brain regeneration

We have introduced a neurologic examination system that is often used to evaluate the motor functional recovery to assess functional rehabilitation at two, four, and eight weeks postoperatively[27]. Rats were suspended one meter above the floor and observed the forelimb flexion. Rat that extended both forelimbs towards the floor was considered no defect and scored 0 point. Rat that has persistent flexion of forelimb on the contra side of surgery but no other disabilities was scored 1 point. Then rats were placed on a platform with strong friction to confirm they can grip the surface by their claws. After placing the rat on the platform slightly lifted the tail by one hand then a mild force was given behind the rat's shoulder as far as the forelimb slid some distance. Then the test was repeated in every direction. If the rat showed reduced resistance to lateral force towards the paretic side we scored 2 points. Rat was set freely on the platform if it has circling movement we scored 3 point. During the observation the forelimb flexion should be observed when assessed force resistance. Homoplastically, both forelimb flexion and decrease of force resistance should be assessed when evaluated circling movement.

2.5 Histological assessment

The rats were sacrificed immediately after the functional assessment and implanted scaffolds were harvested. The animals were anesthetized with 0.5ml/100g body weight 10% chloral hydrate (*ip*) before operation. Then they were perfused with

PBS (PH 7.4) and their cerebrums were collected and frozen in O.C.T (SAKURA, Japan) embedding medium at -80°C. The frozen tissue was cut into 5μm section by cryostat microtome (Thermo Fisher Scientific, USA). The tissue sections were fixed by 4% paraformaldehyde (PH 7.4) for 1 hour. Then they were washed by PBS (PH 7.4) twice and treated with cell permeabilizing solution 0.3% Trition X-100 (Sigma, USA) for 15min. After washed by PBS (PH 7.4) the tissue sections were blocked in immuno staining blocking buffer (B600060, Proteintech, USA) for 60min at room temperature. Then the tissue sections were incubated with anti-GAP43 antibody (ab16053, Abcam, USA, 1:500) and anti-Synaptophysin antibody (SY38, ab8049, Abcam, USA, 1:20) at 4°C overnight. The tissue sections were subsequently reacted with the fluoresceinisothiocyanate (FITC) labeled secondary antibody goat anti-mouse IgG (A0568, Beyotime, China, 1:500) and Cy3 labeled secondary antibody goat anti-rabbit IgG (A0516,Beyotime, China, 1:500) for 1 hour at room temperature and stained with DAPI (0.5μg ml^{-1}) for 10 min at room temperature. The tissue sections were mounted with antifade mounting medium (Beyotime P0126, China) and viewed under CLSM (TCS SP8, Leica, Germany). The remanent brain tissue was routinely embedded by paraffin wax and was cut into 5μm section by microtome (Leica, Germany). Both paraffin tissue sections and frozen tissue sections were routinely stained with hematoxylin and eosin and observed morphology by light microscope (Leica, Germany).

2.6 Western blot

Tissue was harvested after perfused with PBS (PH 7.4), then the scaffold and its

ambient part has been cut off and pulverized in liquid nitrogen. The tissues were lysed in RIPA lysis buffer (Beyotime, China) with phenylmethanesulfonyl fluoride (PMSF, 5μl/ml, Beyotime, China). Protein concentrations were measured with bicinchoninic acid (BCA) protein assay kit (Beyotime, China). Proteins extracts were mixed with sodium dodecyl sulfate-polyacrylamide gel electrophoresis (SDS-PAGE) loading buffer (250μl/ml, solarbio, China) and denatured at 100°C for 10 min and separated on 12% SDS-PAGE at 120 volts for about 1h. Proteins were then transferred to polyvinylidene fluoride (PVDF) membrane, PVDF membrane was washed by tris buffered saline (TBS) and blocked with 5% non-fat milk for 2h at room temperature. The anti-GAP43 antibody (ab16053, Abcam, USA, 1μg/ml) and anti synaptophysin antibody (ab8049, Abcam, USA, 1:500) were added respectively as primary antibodies. The membranes were incubated at 4°C overnight. After washed by mixture of tris-Buffered Saline and tween-20 (TBST) for three times, the membranes were incubated with HRP-labeled goat anti-rabbit IgG (A0208, Beyotime, China) and HRP-labeled goat anti-mouse IgG (A0216, Beyotime, China) for 1.5h. Then the optical density was analyzed by Transilluminator 2020D Gel Pro 4400 (Technology Institute, Beijing, China).

2.7 Statistical analysis

Statistical significance was determined using one-way ANOVA and student's *t* test for multiple comparison tests. Statistical software SPSS 17.0 (Chicago, USA) was used for statistical analysis. $P<0.05$ was considered statistically significant.

3. Result and discussion

3.1 Waterborne Biodegradable Polyurethane (WBPU) 3-Dimentional porous scaffold Preparation and characterizations

Waterborne biodegradable polyurethane (WBPU) was synthesized from PCL and PEG and reacted chain extending reaction with PDO. Then prepolymer was emulsified by L-lysine (See the ECI for detailed information). The 3D structure was formed by freeze-drying method. The WBPU 3D scaffolds showed thickness about 3mm. The SEM result showed well distributed porous structure of WBPU 3D scaffold, the porosity of WBPU17 scaffold is 83.29±0.53%, the porosity of WBPU25 scaffold is 86.72±0.78%. The mean pore size of WBPU17 and WBPU25 scaffold is 20.10μm and 22.18μm respectively (Fig1). Biodegradable polymers such as PCL scaffold have been used widely in nerve tissue engineering[9, 28]. It has fine biocompatibility, but its poor nature of mechanical property and hydrophobicity has limited its application[29]. Here we have introduced PEG which could improve hydrophilicity, pore size and porosity of scaffolds to synthesized non-toxic waterborne biodegradable polyurethane (WBPU) emulsions[24]. We have also applied different molar content of PEG to modify the porosity, pore size and hydrophilicity of scaffolds[24]. Clearly, too high hydrophilicity of biomaterials for tissue engineering applications is not beneficial for cell adhesion, but the degradation rate will decline with low hydrophilicity[21, 25, 30]. Thus, in this study, WBPU17 and WBPU25 that have moderate hydrophilicity, have been applied into the therapy of rat's TBI model[25]. More importantly, no organic solvent has been employed in the whole synthetic process of these WBPU, which can decrease the

toxicity of the process of preparing porous scaffold to a greater degree[24,25]. For the tissue regeneration, it is important to have a suitable pore size to allow cells migration into the pores of scaffold and give an ideal environment for cell nourishment and waste removal[31]. Our scaffolds have the mean pore size of 20.10μm and 22.18μm respectively, which can give enough interspace for neurocyte to infiltrate and proliferate. The 3D structure can give enough superficial area for neural cellular attachment, proliferation, and support the regenerated nerve. It also gives the desired meshy structure as a structural cue for axon reconnection. In our previous study, we have proved WBPU 3D scaffold could provide an ideal environment for angiogenesis[24], which can facilitate regenerative cell to obtaining nourishment and removing metabolic wastes. These results indicate that WBPU 3D scaffold is a promising artificial nerve scaffold that is easy to be prepared. The WBPU 3D scaffold has potential to provide a proper environment for neural cellular attachment, proliferation and metabolism.

3.2 In vitro cell reactions

The rat glial cells were seeded in 96-well plates at the density of 5×10^3 cells per well with different concentrations of degradation liquid to estimate the cytotoxicity of degradation product of WBPU. Results showed that within the logarithmically diluted degradation liquid of WBPU from concentrations of 100% to 0.1%, only 100% concentration of degradation liquid group showed statistical significant difference between the experiment and saline group. Other groups showed no statistical significant difference compared to the saline group (Fig2). Comparison between

WBPU17 group and WBPU25 group displayed no statistical significant difference. It is believed that one important parameter to evaluate safety and availability of biodegradable scaffold is the cytotoxicity of the material and its degradation product[9]. In this experiment, absorbance of formazan product at 450 nm refers to survival rate of cells. Higher absorbance rate refer to preferable cell survival and activity. In our study, only 100% concentration of degradation liquid showed statistical significant difference compared with the experiment and saline groups. But in intracorporeal condition, the WBPU 3D scaffold will degrade gradually and the degradation liquid of WBPU 3D scaffold will not reach such high concentration. Hence, the results of cytotoxicity of degradation product of WBPU indicate that WBPU 3D scaffold has very low cytotoxicity. This result further proves that the WBPU 3D scaffold is cell compatible; it can be applied as neural scaffold in animal research.

3.3 Functional recovery

We have designed a new kind of TBI animal model to achieve the purpose of both tissue damnification and functional impairment. We resected rat's M1 area which is the motor center of rat's forelimb (Fig3). Thus we could cause both cerebral injury and paralysis of rat simultaneously. During the experiment period two rats in the WBPU25 scaffold treated group, one rat in the WBPU17 scaffold treated group and three rats in the saline group died after operation because of brain hernia. The rest of rats were in good condition, no rat showed infection or wound complications. At predetermined time point (two, four, eight weeks postoperatively), the functional recovery was determined by the mean score of neurologic examination system. The

mean point of rat's forelimb motor functional recovery showed obvious rehabilitation of motor function in WBPU17 and WBPU25 scaffold treated group, while the WBPU25 scaffold treated group showed better performance (Fig4).The neurological score system is wildly accepted scale to evaluate the motor functional recovery especially the forelimb motor function[32-34]. Probably, WBPU17 scaffold and WBPU25 scaffold could be degraded gradually, still maintain the intact structure during regeneration of brain tissue process to support the cellular infiltration, axonal regeneration and synaptic reconstruction. In addition, WBPU25 scaffold showed more hydrophilic and porous property than those of the WBPU17 scaffold, hence these may give better support for regeneration and be more suitable for cellular proliferation and axonal reconstruction. These results indicate that WBPU 3D scaffold can improve recovery of motor function.

3.3 Histological assessment

In this study, we collected the brain tissue from rats at two, four and eight weeks after the operation, respectively. The neuronal growth associated protein (GAP43) and synaptophysin (SY38) have been applied to determine regeneration effects of axon and synapse after implanting the WBPU 3D scaffolds. After four weeks, GAP43 was expressed higher for the WBPU25 scaffold treated group than that of the WBPU17 scaffold treated group. Furthermore, they were both strongly expressed compared with the saline group (Fig5). The expression of GAP43 at eight weeks was partly increased in WBPU17 scaffold treated group compared to four weeks result, while expression of GAP43 was still obvious in WBPU25 scaffold treated group.

The expression of synaptophysin showed no obvious difference between WBPU25 scaffold and WBPU17 scaffold treated group at four weeks after implantation. After eight weeks the synaptophysin was strongly expressed in WBPU25 scaffold treated group in comparison with the WBPU17 scaffold treated group, while the saline group showed the weakest expression (Fig6).

During the elongation of axon and formation of synapse, GAP43 is believed to be an important maker of neuroregeneration and strongly expressed at the early stage after injury[35-38]. Thus, GAP43 expression at four weeks indicates the beginning of axonal and synaptic restoration[38]. Since this GAP43 is located on the membrane of differentiated neuron which has started axonal growth. The GAP43 is concentrated in a structure called "growth cone" which will elongate to axon, where the GAP43 will guide expansion of cell membrane through membrane skeleton protein mediated endocytosis to promote growth of axon[39, 40]. WBPU 3D scaffolds have high porosity that can provide large superficial area for attachment of cell membrane. Hence, WBPU 3D scaffolds can give an appropriate environment for growth cone to adhesion and prolongation. Besides, WBPU 3D scaffolds can mimic the extracellular matrix to convenient for membrane skeleton protein attachment and enhance cellular nourishment. WBPU25 scaffold, as mentioned, are more hydrophilic and porous than the WBPU17 scaffold, hence WBPU25 scaffold may provide a wider surface for cellular proliferation.

Synaptophysin is a maker that represents synapses and reconstruction of synapses[41, 42]. Its density is associated with the number of synapses and itself is an

important component of synapses[43-45]. The expression of synaptophysin at eight weeks suggests that synapses were regenerated, which is good agreement with the expression trend of GAP43. Reconstruction of synapses was believed to be associated with functional recovery. Synaptic remodeling is the structural foundation for functional rehabilitation, and the recovery of rat's motor function is closely correlated to reconstruction of synapses[38, 42]. This result further proved that WBPU 3D scaffolds, not only acted as a structural cue to both histic regeneration and axonal regeneration, but also could assist reconstruction of synapses resulting in functional recovery. The results of expression of GAP43 and synaptophysin suggested that the WBPU 3D scaffold was conducive to regeneration of axon and reconstruction of synapses, thus to promote rehabilitation of motor function.

HE staining was employed to assess the general regeneration morphology images in WBPU 3D scaffold at eight weeks postoperative. These results showed that the cells and nerve fibers were rapidly grown into the scaffold from the border to the middle (Fig S2), and infiltrations of blood vessels were observed (Fig7). The WBPU 3D scaffolds were degraded duly, and the boundaries between tissue and scaffold were barely distinguishable at eight weeks after operation (Fig S2). No inflammatory signs or adverse tissue reactions have been seen at implantations (Fig S2), which corroborates the biocompatibility and low toxicity of scaffolds. Ideally, the scaffold should be degraded progressively and replaced by the regenerating tissue gradually[9]. Undoubtedly, the WBPU 3D scaffolds here exhibited ideal features as biodegradable scaffolds, the angiogenesis can facilitate cellular metabolism and nutrition uptake in

scaffold.

3.4 Western blot

To further confirm the expression level of GAP43 and synaptophysin, their expression has been evaluated by the western blot. Expression of GAP43 displayed sustained increase in WBPU25 scaffold treated group at four and eight weeks after implantation. While GAP43 expression in WBPU17 treated scaffold group was increased at eight weeks postoperative. Overall, GAP43 in both scaffold treated groups showed stronger expression than that in saline group at four weeks and eight weeks postoperatively. The expression of synaptophysin showed imperceptible difference at four weeks in WBPU25 and WBPU17 scaffold treated groups. But stronger expression of synaptophysin has been detected in WBPU25 scaffold treated group at eight weeks than that in WBPU17 scaffold treated group. Overall, synaptophysin in both groups showed stronger expression than that in saline group at eight weeks after implantation (Fig 8).

The consistence of western blot and immunofluorescence results further proved the effect of WBPU scaffolds on treatment of TBI. The trend of GAP43 expression and synaptophysin indicates continuous repair of brain tissue and axon in WBPU25 scaffold treated group from four weeks to eight weeks postoperatively. But in the WBPU17 scaffold treated group, the regeneration process dropped off at eight weeks after surgery. We suspected that more acid metabolites might impede nerve generation in WBPU17 scaffold group. The exact mechanism of this phenomena needs further investigation in our ongoing work.

4. Conclusion

Waterborne biodegradable polyurethane 3-dimentional porous scaffold is one kind of porous scaffold prepared based on PCL and PEG. It shows proper porosity, low cytotoxicity, satisfactory hydrophilicity and biodegradability. WBPU 3D scaffolds have axonal and synaptic regeneration ability without any NGF. Both WBPU17 and WBPU25 scaffolds showed favorable nerve regeneration performance with axonal regeneration, synaptic reconstruction and motor functional recovery, while WBPU25 scaffold is better. We demonstrated that WBPU 3D scaffold had axonal and synaptic regeneration abilities in SD rat's TBI model for the first time. Our study proves that WBPU 3D scaffolds, especially WBPU25 scaffolds have fine effect on nerve regeneration and neurological functional recovery. Therefore, WBPU 3-Dimentional porous scaffold has the potential to be applied as a therapeutic implant in brain tissue damage repair, and can promote rehabilitation of neurological deficits after surgery.

Acknowledgements

We would like to thank the financial supports by the National Natural Science Foundation of China (contract/grant number: 81100925, 81472361, 51273124, 51273126) and the National Science Fund for Distinguished Young Scholars of China (contract/grant number: 51425305)

Conflict of interest

The authors declare no competing financial interest.

References:

1. J. Ghajar, *Lancet (London, England)*, 2000, **356**, 923-929.
2. N. Andelic, *Lancet neurology*, 2013, **12**, 28-29.
3. J. V. Rosenfeld, A. I. Maas, P. Bragge, M. C. Morganti-Kossmann, G. T. Manley and R. L. Gruen, *Lancet (London, England)*, 2012, **380**, 1088-1098.
4. L. C. Piper, C. K. Zogg, E. B. Schneider, J. A. Orman, T. E. Rasmussen, L. H. Blackbourne and A. H. Haider, *JAMA surgery*, 2015, DOI: 10.1001/jamasurg.2015.1838.
5. D. J. Cooper, J. V. Rosenfeld, L. Murray, Y. M. Arabi, A. R. Davies, P. D'Urso, T. Kossmann, J. Ponsford, I. Seppelt, P. Reilly and R. Wolfe, *The New England journal of medicine*, 2011, **364**, 1493-1502.
6. J. P. Niemeier, L. M. Grafton and T. Chilakamarri, *North Carolina medical journal*, 2015, **76**, 105-110.
7. L. Aloe, M. L. Rocco, P. Bianchi and L. Manni, *J Transl Med*, 2012, **10**, 239-239.
8. A. I. Ahmed, S. Gajavelli, M. S. Spurlock, L. O. Chieng and M. R. Bullock, *Journal of the Royal Army Medical Corps*, 2015, DOI: 10.1136/jramc-2015-000475.
9. G. A. Saracino, D. Cigognini, D. Silva, A. Caprini and F. Gelain, *Chemical Society Reviews*, 2013, **42**, 225-262.
10. S. Hou, Q. Xu, W. Tian, F. Cui, Q. Cai, J. Ma and I.-S. Lee, *Journal of neuroscience methods*, 2005, **148**, 60-70.
11. Y. Wei, W. Tian, X. Yu, F. Cui, S. Hou, Q. Xu and I.-S. Lee, *Biomedical Materials*, 2007, **2**, S142.
12. W. Tian, S. Hou, J. Ma, C. Zhang, Q. Xu, I. Lee, H. Li, M. Spector and F. Cui, *Tissue engineering*, 2005, **11**, 513-525.
13. R. G. Ellis-Behnke, Y. X. Liang, S. W. You, D. K. Tay, S. Zhang, K. F. So and G. E. Schneider, *Proceedings of the National Academy of Sciences of the United States of America*, 2006, **103**, 5054-5059.
14. W. Wang, S. Itoh, A. Matsuda, T. Aizawa, M. Demura, S. Ichinose, K. Shinomiya and J. Tanaka, *Journal of Biomedical Materials Research Part A*, 2008, **85**, 919-928.
15. S. Y. Chew, R. Mi, A. Hoke and K. W. Leong, *Advanced Functional Materials*, 2007, **17**, 1288-1296.
16. S. Panseri, C. Cunha, J. Lowery, U. Del Carro, F. Taraballi, S. Amadio, A. Vescovi and F. Gelain, *Bmc Biotechnology*, 2008, **8**, 39.
17. K. I. Park, Y. D. Teng and E. Y. Snyder, *Nature biotechnology*, 2002, **20**, 1111-1117.
18. M. Maitz, *Biosurface and Biotribology*, 2015, **1**, 161-176.
19. J. I. Kim, H. R. Pant, H.-J. Sim, K. M. Lee and C. S. Kim, *Materials Science and Engineering: C*, 2014, **44**, 52-57.
20. A. T. Stevenson, L. M. Reese, T. K. Hill, J. McGuire, A. M. Mohs, R. Shekhar, L. R. Bickford and A. R. Whittington, *Biomaterials*, 2015, **54**, 168-176.
21. H. Janik and M. Marzec, *Materials Science and Engineering: C*, 2015, **48**, 586-591.
22. T. Hausner, R. Schmidhammer, S. Zandieh, R. Hopf, A. Schultz, S. Gogolewski, H. Hertz and H.

Redl, *Acta neurochirurgica. Supplement*, 2007, **100**, 69-72.
23. Y. Niu, K. C. Chen, T. He, W. Yu, S. Huang and K. Xu, *Biomaterials*, 2014, **35**, 4266-4277.
24. X. Jiang, F. Yu, Z. Wang, J. Li, H. Tan, M. Ding and Q. Fu, *Journal of Biomaterials Science, Polymer Edition*, 2010, **21**, 1637-1652.
25. Z. Wang, L. Yu, M. Ding, H. Tan, J. Li and Q. Fu, *Polymer Chemistry*, 2011, **2**, 601-607.
26. P. George and W. Charles, *Qingchuan Zhuge translate)(People's Medical Publishing House, Beijing, China, 2007)*, 1998, **32**.
27. J. B. Bederson, L. H. Pitts, M. Tsuji, M. Nishimura, R. Davis and H. Bartkowski, *Stroke; a journal of cerebral circulation*, 1986, **17**, 472-476.
28. J. Xie, M. R. MacEwan, A. G. Schwartz and Y. Xia, *Nanoscale*, 2010, **2**, 35-44.
29. H. Zhang and A. I. Cooper, *Advanced materials*, 2007, **19**, 1529-1533.
30. G.-E. Chen, L. Sun, Z.-L. Xu, H. Yang, H.-H. Huang and Y.-J. Liu, *Korean Journal of Chemical Engineering*, 2015, 1-9.
31. A. F. Quigley, J. M. Razal, B. C. Thompson, S. E. Moulton, M. Kita, E. L. Kennedy, G. M. Clark, G. G. Wallace and R. M. Kapsa, *Advanced Materials*, 2009, **21**, 4393.
32. X. Pang, T. Li, L. Feng, J. Zhao, X. Zhang and J. Liu, *Journal of pharmacological and toxicological methods*, 2014, **69**, 217-222.
33. M. Y. Mahat, N. Fakrudeen Ali Ahamed, S. Chandrasekaran, S. Rajagopal, S. Narayanan and N. Surendran, *J Neurosci Methods*, 2012, **211**, 272-279.
34. L. S. Machado, I. Y. Sazonova, A. Kozak, D. C. Wiley, A. B. El-Remessy, A. Ergul, D. C. Hess, J. L. Waller and S. C. Fagan, *Stroke; a journal of cerebral circulation*, 2009, **40**, 3028-3033.
35. P. J. Meberg, C. A. Barnes, B. L. McNaughton and A. Routtenberg, *Proceedings of the National Academy of Sciences*, 1993, **90**, 12050-12054.
36. D. Carulli, A. Buffo and P. Strata, *Progress in neurobiology*, 2004, **72**, 373-398.
37. J. Piontek, A. Regnier-Vigouroux and R. Brandt, *Journal of neuroscience research*, 2002, **67**, 471-483.
38. N. Rosskothen-Kuhl and R. B. Illing, *PloS one*, 2014, **9**, e92624.
39. A. Gauthier-Kemper, M. Igaev, F. Sundermann, D. Janning, J. Bruhmann, K. Moschner, H. J. Reyher, W. Junge, K. Glebov, J. Walter, L. Bakota and R. Brandt, *Molecular biology of the cell*, 2014, **25**, 3284-3299.
40. D. Frey, T. Laux, L. Xu, C. Schneider and P. Caroni, *The Journal of cell biology*, 2000, **149**, 1443-1454.
41. G. Thiel, *Brain Pathology*, 1993, **3**, 87-95.
42. X. E. Hou and A. Dahlstrom, *Neurochemical research*, 2000, **25**, 1275-1300.
43. K. Algarrahi, D. Franck, C. E. Ghezzi, V. Cristofaro, X. Yang, M. P. Sullivan, Y. G. Chung, S. Affas, R. Jennings, D. L. Kaplan, C. R. Estrada, Jr. and J. R. Mauney, *Biomaterials*, 2015, **53**, 149-159.
44. O. H. Shin, *Comprehensive Physiology*, 2014, **4**, 149-175.
45. B. Granseth, B. Odermatt, S. J. Royle and L. Lagnado, *The Journal of physiology*, 2007, **585**, 681-686.

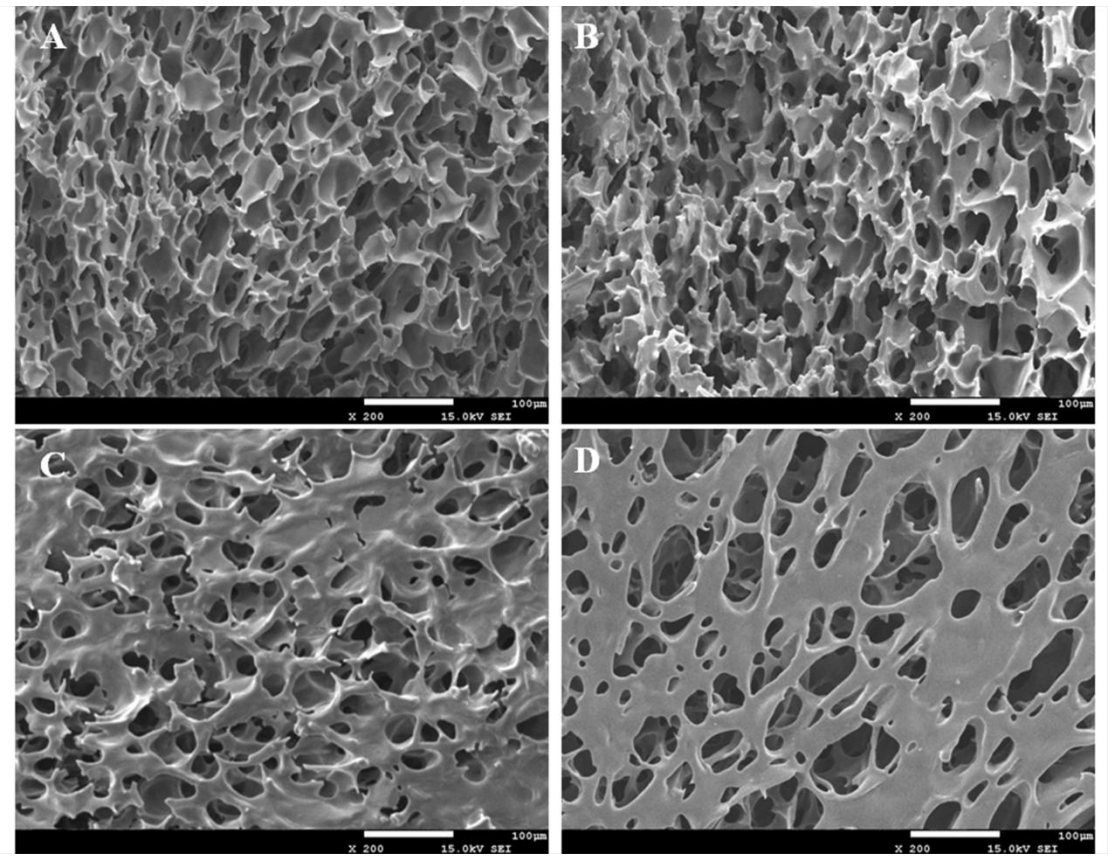

Figure1. SEM morphology of interconnected waterborne biodegradable polyurethane (WBPU) 3-Dimentional porous scaffolds. Scale bars: 100μm. Cross-section morphology of WBPU17 (A), WBPU25 (B). Surface morphology of WBPU17(C), WBPU25 (D).

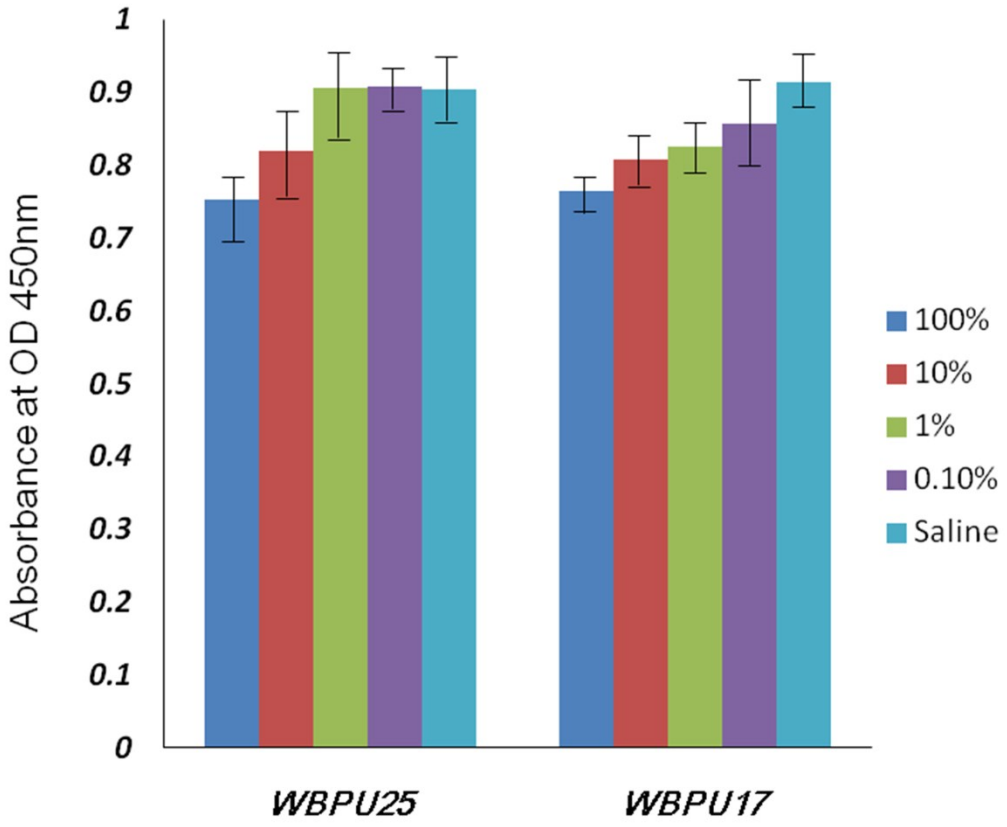

Figure2. Absorbance profiles of formazan products were tested at OD 450nm to reflect cytotoxicity of degradation liquid of WBPU in rat's glial cell. Cell absorbance at 100% concentration of degradation liquid was lower than those of other experiment groups and saline group ($P<0.05$). There was no statistical difference between WBPU25 treated group and WBPU17 treated group at same concentration ($P>0.05$).

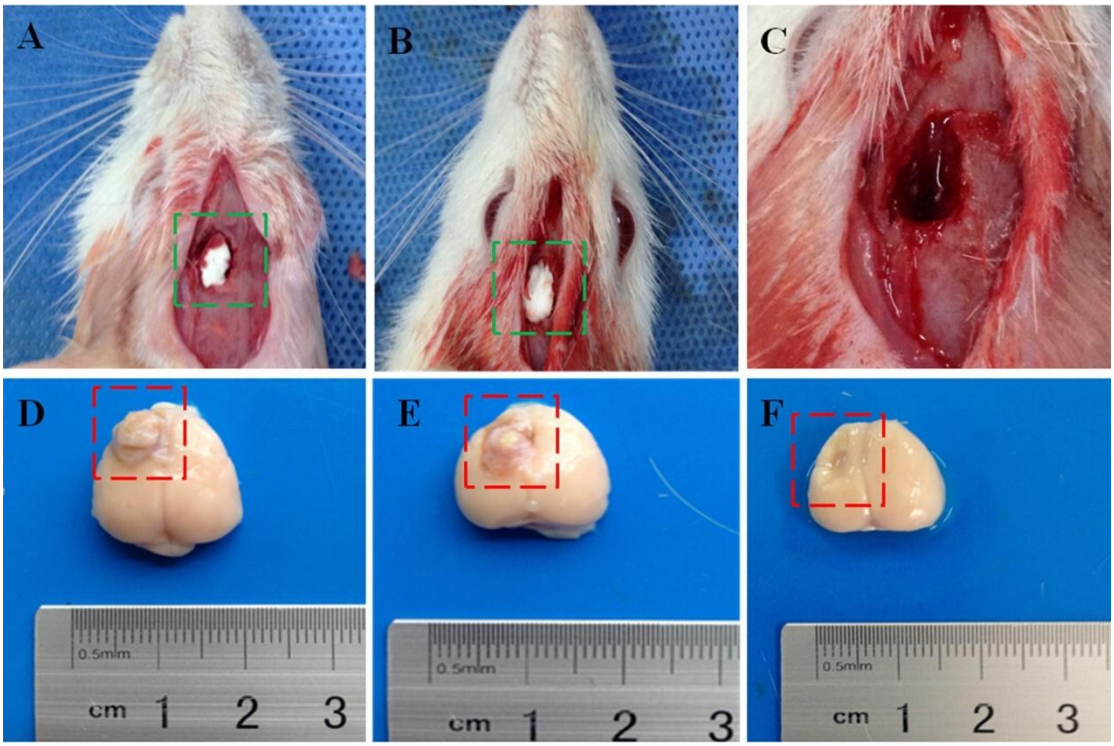

Figure3. Morphology of WBPU 3D scaffolds before and after implanted in rats' TBI model. The M1 was resected and the tissue defects were filled by WBPU25 scaffold (A, marked by the green frame), WBPU17 scaffold (B, marked by the green frame) and saline (C), respectively. The figure of saline group (C) was magnified to show tissue defect. The tissue defects were restored in WBPU25 scaffold (D, marked by the red frame) and WBPU17 scaffold (E, marked by the red frame) treated groups after eight weeks postoperatively. In saline treated group tissue defect was still distinguishable (F, marked by the red frame) at the same time.

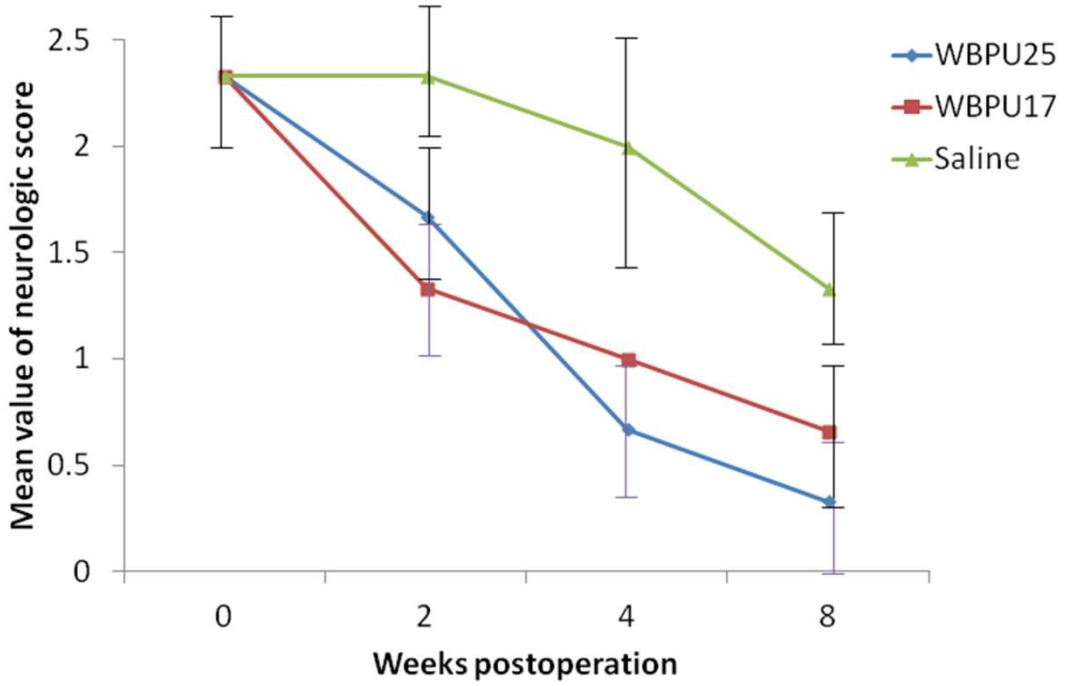

Figure4. The neurologic score of rats' TBI model after implanted WBPU 3D scaffold and saline at two, four, and eight weeks. WBPU17 and WBPU25 scaffold treated groups showed better recovery of motor function than saline treated group. n=3; $P<0.05$

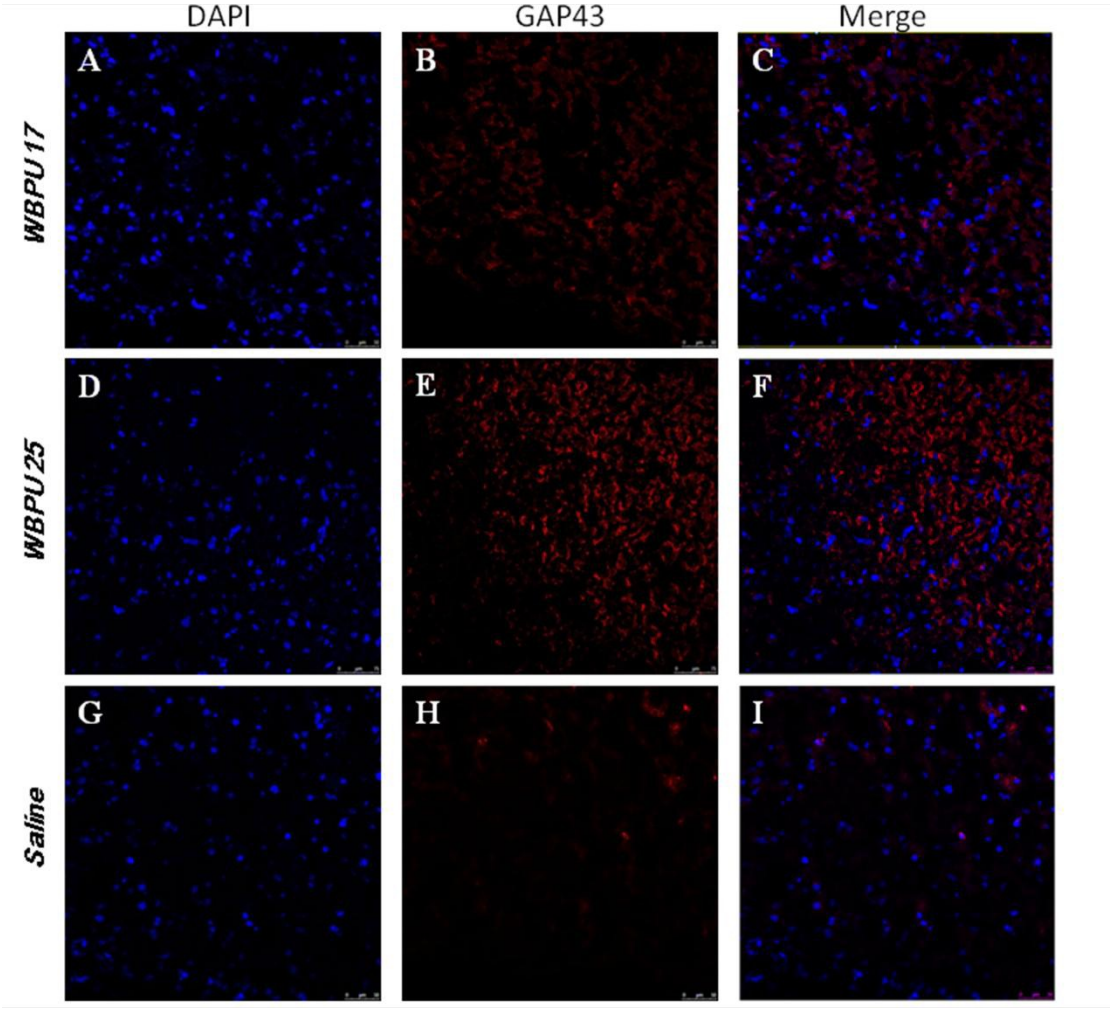

Figure5. The CLSM images show effect of axonal regeneration on the rats' TBI model at four weeks after implanted WBPU 3D scaffold. The immunofluorescence assay shows the neurite outgrowth. Scale bars: 50μm. DAPI stained the nucleolus (right panel A, D, G) GAP43 stained the neurite outgrowth (middle panel B, E, H) and they were merged in the right panel(C, F, I).

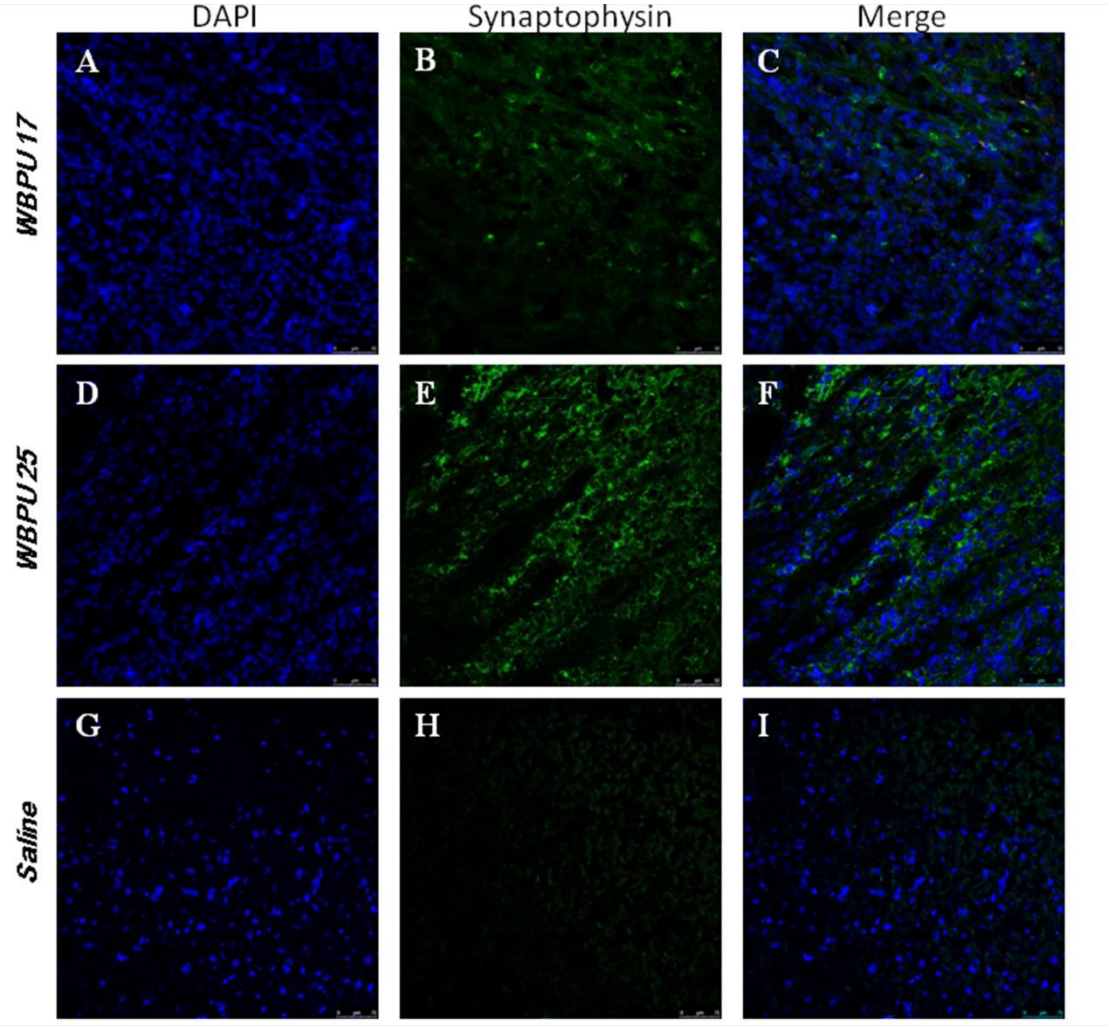

Figure6. The CLSM images show effect of synapse reconstruction on the rats' TBI model at eight weeks after implanted WBPU 3D scaffolds. The immunofluorescence assay shows the synapse. Scale bars: 50μm. DAPI stained the nucleolus (right panel A,D,G), synaptophysin stained the reconstructed synapse (middle panel B,E,H) and they were merged in the right panel (C,F,I).

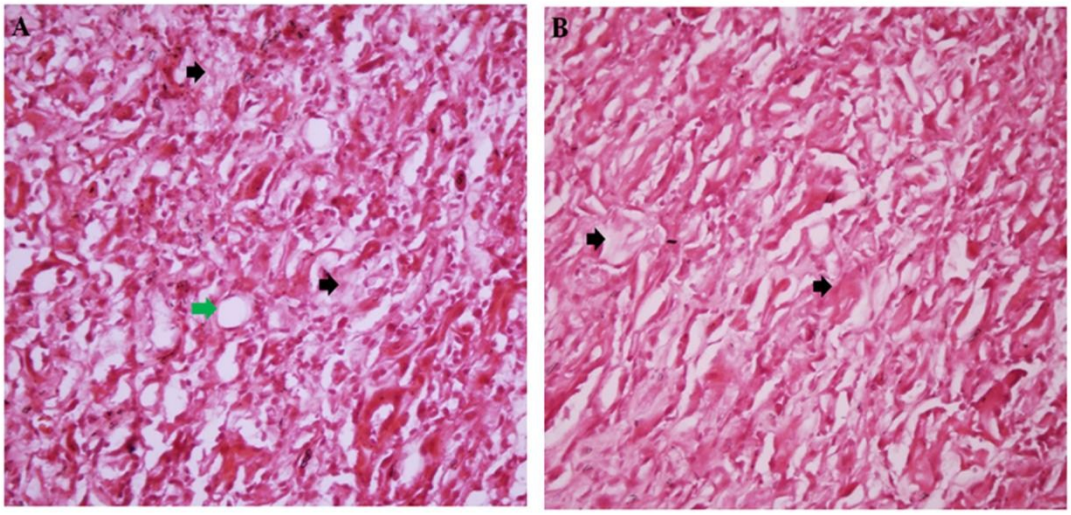

Figure7. HE stained rats' brain tissues at magnification of 400X. HE images show the infiltration of cells into the WBPU 3D scaffolds and degradation of WBPU 3D scaffolds at eight weeks postoperatively. The figures show infiltration of cells and degradation of WBPU25 scaffold (A) and WBPU17 scaffold (B), respectively. Green arrow, blood vessel; black arrow, degrading scaffold.

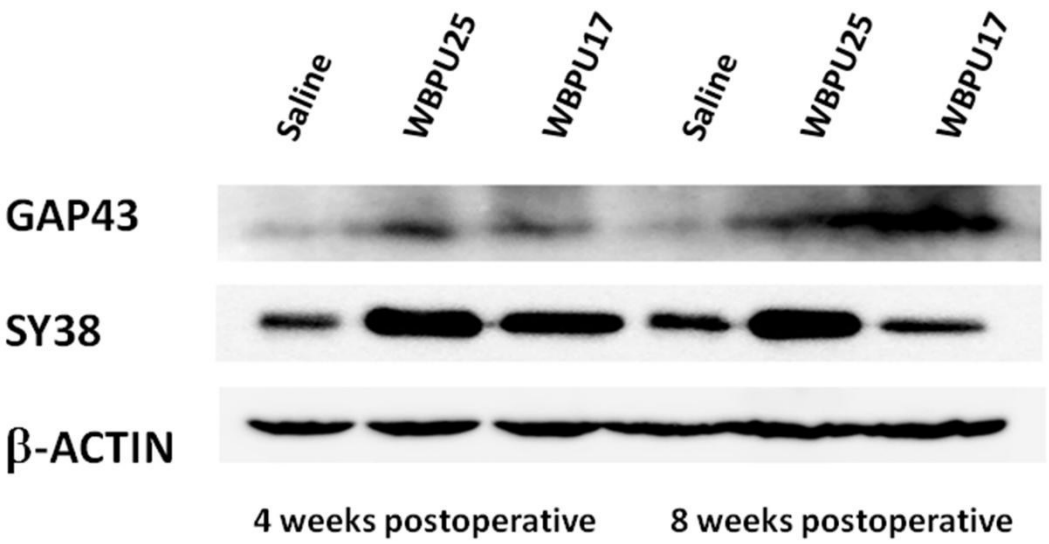

Figure8: Western blot shows continually increased expression of GAP43 in WBPU25 scaffold treated group at four and eight weeks after implantation. Expression of GAP43 in WBPU17 scaffold treated group was increased at eight weeks after implantation. Both of them have stronger expression of GAP43 than that of saline treated group. Expression of synaptophysin at eight weeks after implantation was stronger in WBPU25 scaffold treated group than that in WBPU17 scaffold treated group. Both of them have stronger expression than that in saline treated group.

Table of contents entry

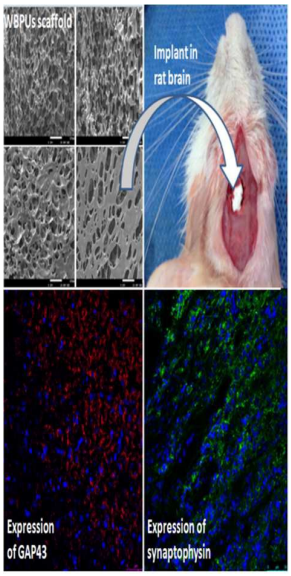

It was demonstrated for the first time that WBPU 3D scaffold had axonal and synaptic regeneration abilities in rat brains.